SAND92-2890
Unlimited Release
Printed January 1993

Distribution
Category UC-126

Bayou Choctaw Caverns 15 and 17 Web Analysis

Brian Ehgartner
Underground Storage Technology Department
Sandia National Laboratories
Albuquerque, New Mexico

ABSTRACT

The relatively thin web of salt that separates Bayou Choctaw Caverns 15 and 17 was evaluated using the finite-element method. The stability calculations provided insight as to whether or not any operation restrictions or recommendations are necessary. Because of the uncertainty in the exact dimensions of the salt web, various web thicknesses were examined under different operating scenarios that included individual cavern workovers and drawdowns. Cavern workovers were defined by a sudden drop in the oil side pressure at the wellhead to atmospheric. Workovers represent periods of low cavern pressure. Cavern drawdowns were simulated by enlargening the cavern diameters, thus decreasing the thickness of the web. The calculations predict that Cavern 15 dominates the behavior of the web because of its larger diameter. Thus, given the choice of caverns, Cavern 17 should be used for oil withdrawal in order to minimize the adverse impacts on web resulting from pressure drops or cavern enlargement. From a stability point of view, maintaining normal pressures in Cavern 15 was found to be more important than operating the caverns as a gallery where both caverns are maintained at the same pressure. However, during a workover, it may be prudent to operate the caverns under similar pressures to avoid the possibility of a sudden pressure surge at the wellhead should the web fail.

CONTENTS

FIGURES

TABLES

1.0 INTRODUCTION

The Strategic Petroleum Reserve (SPR) was created to reduce the vulnerability of the United States to interruptions by foreign oil suppliers. Approximately 570 million barrels (MMB) of crude oil are presently stored underground in salt domes at five sites located along the Gulf of Mexico. Most of the crude oil is stored in leached caverns.

The initial caverns, known as Phase I, were acquired rather than leached anew. As a result, some of the cavern spacings were closer than would now be recommended under the design guidelines for new caverns (SPR, 1987). Bayou Choctaw Caverns 15 and 17 were among those caverns acquired during the development of the SPR. A relatively thin web of salt separates the caverns and there is uncertainty regarding the thickness of the web. As such, the manner in which the caverns are operated is affected. A large pressure differential across the web could cause the caverns to communicate and possibly the web to rupture.

The stability of the web of salt that separates Bayou Choctaw Caverns 15 and 17 was evaluated using the finite-element method. The calculations provide insight as to whether or not any operational restrictions or recommendations are necessary. Because of the uncertainty in the exact dimensions of the salt web and in the future operations of the caverns, various web thicknesses were examined under different operating scenarios that included individual cavern workovers and drawdowns. Cavern workovers were defined by a sudden drop in the oil side pressure at the wellhead to atmospheric and thus represent periods of low cavern pressure. Cavern drawdowns were simulated by enlargening the cavern diameters, thus decreasing the thickness of the web from 156 ft to only 56 ft.

Previous elastic-plastic web analyses (Ney, 1979; and Hilton, Tillerson, Benzley, and Gubbels, 1980) of the caverns predicted potential tensile failure in the web due to uneven loading across the web. However, the analyses did not include a creep constitutive model for salt and simulated the loading as instantaneous. This work was done prior to the

development of a creep model and laboratory testing of Bayou Choctaw salt properties.

The updated analyses presented in this report use the M-D salt creep model (Munson, et al., 1989a) with Bayou Choctaw salt specific properties, apply time-dependent loading cycles, and include a compressive failure criterion based upon the accumulated inelastic strain (**Preece** and Wawersik, 1984).

2.0 FINITE-ELEMENT MODEL

The site layout at Bayou Choctaw is shown in Figure 1. Of particular interest are the location of Caverns 15 and 17 relative to each other, their neighbors, and the edge of the dome. These distances are needed to define the boundaries of the finite-element model.

Figure 2 shows an east-west vertical cross-section through Caverns 15 and 17. There is uncertainty as to the exact cavern dimensions and web thickness and they both vary with depth. The values used in this study approximate averages and are based on Figure 2. The caverns are spaced 460 ft center-to-center. Cavern 15 has a diameter of approximately 430 and Cavern 17 has a diameter of approximately 177 ft in its upper portion. The resulting web of salt separating the two caverns is initially 156 ft thick and will decrease to 56 ft after 6 drawdowns-- 3 for each cavern. This range in web thickness should cover the possibilities. Some estimates place the caverns within 110 ft or less (Neal, Magorian, and Acres, in prep.).

The analysis examines a horizontal cross-section at a depth of 3000 ft below the surface. The finite-element mesh is shown in Figure 3. Given the aspect ratio of the cavern geometries, a plain strain representation was assumed; therefore, the caverns are modeled as infinitely long. At the simulated depth, ‘the distance to the edge of the dome is approximately 1150 ft from the centerline of Cavern 17. At the outer

boundary, a constant lithostatic pressure of 2858 psi was applied. This value was estimated assuming the 637 ft of overburden and caprock material to contribute a stress gradient of 1 psi/ft of depth and the underlying salt a stress gradient of 0.94 psi/ft of depth.

The distance, volumes, and relative depths of the neighboring caverns were used to estimate boundary locations for the model. For purposes of this model, Caverns 4 and 18 located to the south and the UTP and Allied caverns to the north formed a top model boundary at 396 ft from the centers of the caverns. Caverns 2 and 3 located to the west formed a side boundary at 475 ft from the center of Cavern 15. The boundary conditions assigned to the north, south, and west boundaries of the model mechanically represent rollers allowing free displacement parallel to the boundary, but fixed displacement in the normal direction thus restricted salt flow vertically at the boundaries. These boundaries simulate planes of symmetry for both geometry and loading. As such, only 1/2 of the needed cavern geometry is meshed. The simulated geometry idealizes the entire site as 4 infinitely long rows of caverns. The caverns in the center 2 rows are the size of Cavern 15 and the outer 2 rows the size of cavern 17. Since this idealization is not completely accurate, macroscopic (cavern) performance will not be evaluated. Rather, attention will concentrate on the web that separates the caverns.

The first year of simulation gradually lowered the cavern pressure from lithostatic (2860 psi) to the assumed cavern operating pressure (2000 psi at 3000 ft) for each cavern. There is uncertainty in the operating histories of Caverns 15 and 17 as they were created in the mid 1950's and acquired for use by the SPR in the late 1970's and mid 1980's, respectively. While in SPR use, the operating pressure range has narrowed over time. For example, in 1979 the operating pressure range was 384 to 1357 psi wellhead (add 1110 psi for pressure at the 3000 ft deep web) and in recent years 825 to 1000 psi wellhead. Prior to SPR use, the caverns were used for ethane storage with pressures up to 2000 psi at the web. Wellhead pressures for ethane may be calculated by assuming a density gradient of 0.16 psi/ft.

The next 29 years of simulation assumed a constant pressure of 2000 psi for the caverns. This part of the analysis is intended to simulate the maturity of the present day caverns. Next, three 5-year cycles were simulated. This portion of the analysis operationally exercises the caverns. The purpose is to examine the effects of workovers or low periods of pressure and drawdowns on the stability of the web for future operation of the caverns. The workovers create large pressure differentials across the web. The drawdowns, which remove salt, enable the stability of thinner webs to be evaluated. Each cycle has a workover and drawdown associated with each cavern according to Table 1.

Table 1
Cavern Pressure Histories

Time (years)	Cavern 15 Pressure (psi)	Cavern 17 Pressure (psi)	Comments
0	2860	2860	Lithostatic
1 - 30	2000	2000	Average Historic Operating Pressure
30 - 30.25	1110	2000	Workover 15
30.25 - 30.5	2000	2000	
30.5 - 30.75	2000	1110	Workover 17
30.75 - 31	2000	2000	
31	2000	2000	Drawdown 15
31.25	2000	2000	Drawdown 17
35 - 35.25	1110	2000	Workover 15
35.25 - 35.5	2000	2000	
35.5 - 35.75	2000	1110	Workover 17
35.75 - 36	2000	2000	
36	2000	2000	Drawdown 15
36.25	2000	2000	Drawdown 17
40 - 40.25	1110	2000	Workover 15
40.25 - 40.5	2000	2000	
40.5 - 40.75	2000	1110	Workover 17
40.75 - 41	2000	2000	
41	2000	2000	Drawdown 15
41.25	2000	2000	Drawdown 17
45	2000	2000	End of Simulation

Workovers were assumed to have a wellhead pressure of 0 psi (or 1110 psi at 3000 ft) for 3 months. This is a conservative time period if the caverns are repressured via fluid transfer after the workover is complete. Cavern repressurization is the recommended process. If however the caverns are left to repressurize on their own due to the creep of the salt, a longer time period may be required, In these analyses, after 3 months, the caverns were pressured up to the normal operating pressure at a wellhead pressure of 890 psi or 2000 psi at 3000 ft below surface. All pressure drops and increases were stepped over a 1 day period with incremental pressure not exceeding 150 psi. Drawdowns were simulated at a pressure of 2000 psi at the web by removing 1 ring of surrounding elements. The drawdown history and resulting cavern diameters and web thickness are reported in Table 2. Each drawdown was assumed to enlarge the cavern diameter by 10 percent. This value is an average diameter change derived by assuming that seven volumetric units of fresh water dissolve one volumetric unit of salt. In actual practice, the bottom diameter of the cavern may be enlarged to as much as 20 percent with only minor enlargement in the roof area.

Table 2
Enlargement in Cavern Diameters
Due to Leaching During Drawdowns*

Time /Years)	Cavern 15 Diameter (ft)	Cavern 17 Diameter (ft)	Web Thickness (ft)
31	430 to 473		156 to 135
31.25		177 to 195	135 to 126
36	473 to 520		126 to 102
36.25		195 to 214	102 to 93
41	520 to 572		93 to 67
41.25		214 to 236	67 to 56

*Dimensions do not account for creep.

The stability criterionis based on the accumulated effective strain of the salt. For confining pressures above 500 to 870 psi, the maximum allowable strain has been defined as 13.8 to 15.5 percent, respectively

(Krieg, 1984; Munson, 1989; and Preece and Wawersik, 1984). These results are based on the measured strains at yield obtained from laboratory triaxial creep tests on salt. According to the criteria, the maximum allowable strain limit increases with confining pressure. For purposes of evaluating the analyses in this report, where the cavern pressure does not drop below 1110 psi, the maximum allowable accumulated strain is assumed to be 15.5 percent. From this value, a safety factor is defined as simply the ratio of maximum allowable strain (15.5%) to the effective strain in the salt. From this simplistic approach, potential areas of instability can be defined by safety factors less than one.

3.0 CONSTITUTIVE MODEL

The mechanical behavior of the salt was represented by the Munson-Dawson creep model. The model is state-of-art in predicting salt behavior using a first principles approach. The model is presently being validated with underground data from the WIPP and the validation exercises thus far show good to excellent agreement of predicted room closures with underground measurements. The model predictions for SPR subsidence and cavern pressurization rates agree well with those measured at West Hackberry (Ehgartner, 1992).

The model is a Multimechanism Steady-state Workhardening/Recovery Model as originally developed by Munson and Dawson (1979) and later modified to provide a more descriptive transient strain function (Munson, Fossum, and Senseny, 1989a,b). The model incorporates the Tresca flow potential and is based on micromechanistic concepts using a deformation mechanism map (Munson, 1979). The mechanism map defines regions of stress and temperature in which a unique deformation mechanism controls or dominates steady-state creep. The model identifies three steady-state mechanisms. The total steady-state strain rate is simply the sum of the strain rates of each individual mechanism.

$$\dot{\varepsilon}_s = \sum_{1}^{3} \dot{\varepsilon}_{s_i}$$

The equations describing each of the individual steady-state mechanisms follow. Mechanism 1 (dislocation climb) dominates at high temperatures and low stresses. Mechanism 2 (undefined) controls creep at low temperatures and stresses, and Mechanism 3 (dislocation glide) dominates at high stresses at all temperatures.

$$\dot{\varepsilon}_{s_1} = A_1 \, e^{-Q_1/RT} \, (\sigma/\mu)^{n_1}$$

$$\dot{\varepsilon}_{s_2} = A2 \, e^{-Q_2/RT} \, (\sigma/\mu)^{n_2}$$

$$\dot{\varepsilon}_{s_3} = |H| \, [Bl \, e^{-Q_1/RT} + B2 \, e^{-Q_2/RT}] \sinh [q(\sigma-\sigma_0)/\mu]$$

Each of the above mechanisms relates the steady-state strain rate to temperature, T, and stress, σ. The temperature was assumed constant at 115 "F. The constants A, n, Q are determined from laboratory creep tests. Q is the activation energy and n is the stress exponent. R is the universal gas constant and μ is the shear modulus of salt. $|H|$ is the Heaviside step function with argument of (a-00). The basic form of the creep law for steady-state Mechanisms 1 and 2 is similar to that used in previous analyses for both the Waste Isolation Pilot Plant (WIPP) and the SPR (Krieg, 1984).

Transient creep is included in the model through a function composed of a workhardening branch, an equilibrium branch, and a recovery branch. The details of this component and the steady-state component of creep are discussed by Munson, Fossum, and Senseny (1989a). Transient strain rate is related to the steady-state strain rate through the following function:

$$\dot{\varepsilon} = F \, \dot{\varepsilon}_s$$

The transient function, F, is composed of a workhardening, equilibrium, and recovery branch.

$$F = \begin{cases} \exp \Delta \, (1 - \zeta/\varepsilon_t)^2 & \text{Workhardening} \\ 1 & \text{Equilibrium} \\ \exp -6 \, (1 - \zeta/\varepsilon_t)^2 & \text{Recovery} \end{cases}$$

A and δ are workhardening and recovery parameters and ε_t is the transient strain limit. The equation governing the rate of change of the internal variable, ζ, is

$$\dot{\zeta} = (F\text{-}1)\ \dot{\varepsilon}_s$$

The transient strain limit is related to stress and temperature, T, through the following function where K_o, c, and m are constants.

$$\varepsilon_t = K_o\ e^{ct}\ (\sigma/\mu)^m$$

The workhardening and recovery parameters are defined as a function of stress through

$$A== \alpha_w + \beta_w \log(\sigma/\mu)$$
$$\delta = \alpha_r + \beta_r \log(\sigma/\mu)$$

where the o's and β's are constants with the subscripts denoting either the workhardening or recovery branches.

The salt properties in the analyses were based on a series of laboratory creep tests performed on one sample of salt core from Bayou Choctaw (Wawersik and Zeuch, 1984). The measured strain rates from the triaxial laboratory creep tests enable an approximation of the properties of steady-state Mechanism 2. The properties required for Mechanisms 1 and 3 were not available for Bayou Choctaw salt, therefore WIPP properties were used as needed. Mechanisms 1 and 3 are minor contributors to the total creep of the salt given the temperature and stress states in the model. The WIPP properties are from an extensive reevaluation of the WIPP data bases (Munson, Fossum, and Senseny 1989a,b).

The transient properties used in the analysis are important because of the pressure changes exerted on the web during workovers. The values used in the transient portion of the model were also taken from the WIPP data set. But given their importance, the values used in the analyses were verified by comparing the predicted to measured strains of the

triaxial creep test performed on Bayou Choctaw core. Since the laboratory tests include both transient and steady-state strains, the ability to accurately predict both of these can be checked by simulating the laboratory tests. The approach and results of this comparison are more fully discussed in the Appendix to this report. The agreement was excellent, thus providing confidence in the model and its parameters. Table 3 lists the elastic, steady-state creep, and transient creep properties of salt used in the analyses.

Table 3
Mechanical Properties of Bayou Choctaw Salt

Elastic Properties	
Poisson's Ratio	0.25
Modulus of Elasticity (E)	31.0 GPa
Creep Properties	
Steady-state Mechanism 1	
A_1	8.386 E22 /s
Q_1	25000 cal/mol
n_1	5.5
Steady-state Mechanism 2	
A2	8.45 E10 /s
Q_2	11830 cal/mol
"2	4.06
Steady-state Mechanism 3	
B_1	6.086 E6 /s
B2	3.034 E-2 /s
σ_o	20.57 MPa
q	5.335 E3
R	1.987 cal/mol-deg
Transient Creep	
m	3.0
K_0	6.275 E5
c	0.009198 /T
α_w	-17.37
β_w	-7.738
or	-2.69
β_r	-1.00

* Steady-state constants A2, Q_2, n_2 for Mechanism 2 were estimated from laboratory creep tests (Wawersik and Zeuch, 1984). Steady-state parameters for Mechanisms 1 and 3 were taken from the WIPP data base (Munson, 1992) for pure halite. They should have minor effects on the creep of the web given-its temperature and stress states. Transient parameters are also for pure halite from WIPP data base. The above parameters accurately simulated the laboratory creep tests (see Appendix).

The current version of the code does not change the constitutive model or properties if failure is predicted. As a result, the predicted areas of instability are approximate and should be thought of as 'potential' areas of instability. [A new version of the model is under development and should be available for use in 1993. The new model will feature a much more descriptive failure function with various modes of failure, and the ability to simulate progressive failure of the salt through adaptive meshing (Chan, Bodner, Fossum, and Munson, 1992).]

The SPECTROM-32 code (RE/SPEC, 1989), version 4.02, was used to perform the simulations. The code is a two-dimensional finite-element thermomechanical stress analysis program written to solve nonlinear, time-dependent rock mechanics problems.

4.0 RESULTS

The predicted web safety factors for the initial 30 years of the simulation are shown in Figure 4. The first year results are not plotted on the figure. That period approximated the solution mining of the cavern by gradually reducing the cavern pressures from lithostatic to normal operating pressure and the safety factors were quite high. With time, the safety factors at the sides of the web decrease to approximately 5 at 30 years which, for the most part, represents the current age of the caverns. The predicted safety factor along the wall of Cavern 15 (the larger cavern) is slightly higher.

Figure 5 shows the distribution of the safety factor through the web at 30, 30.25, and 30.75 years. These times are intended to correspond to the current mature cavern state (30 yrs.) and immediately after a Cavern 15 workover (30.25 yrs.) and Cavern 17 workover (30.75 yrs.). The figure shows how the safety factor is effected by workovers or periods of low cavern pressure. The most significant reduction is noted when Cavern 15 undergoes a workover. The safety factor reduces from 5.8 to 3.7 next to Cavern 15. The workover of Cavern 17 resulted in very

little change in safety factor, particularly on the opposite side of the web. Thus it would appear that the pressures in Cavern 15 control the stability of the web and a workover or depressurization of that cavern can significantly reduce the safety factor of the web.

In reviewing the stress state in the web, it is noted that the minimum principal stress in the web was predicted to be 690 psi compressive. Thus tensile failure is not predicted in the salt. Further, sufficient confinement is present in the salt that the assumed failure criteria is not violated. As previously discussed, the maximum allowable accumulated strain is a function of confining pressure. The minimum principal stress falls within the assumed range in confining pressures upon which the failure criterion is based. The minimum stress is predicted in the wall of Cavern 15 immediately following a workover of the cavern. During the first workover of Cavern 15, the minimum stress at the wall was predicted to be 1200 psi. The next workover of Cavern 15 resulted in a minimum stress of 850 psi in the wall. The final workover of Cavern 15 had a minimum stress of 690 psi associated with it. It appears that as the web becomes narrower due to the drawdowns, the possibility of a tensile stress state increases, but is not predicted over the web sizes analyzed here (156 to 56 ft). Other 2-D creep analysis (Ratigan and DeVries, 1989) of brine storage in two closely spaced caverns of equal size have predicted tensile failure for pillar-to-diameter ratios of less than 0.2 when one cavern was pressurized up to 90 percent of lithostatic for purposes of cavern certification. A cavern integrity test of Cavern 17 has shown "significant transients due to interactions with Cavern 15" (Goin and Buchanan, 1986), making test interpretation difficult. As a result, the caverns are currently tested at approximately the same web pressure.

Figure 6 plots the predicted safety factor on each side of the web for all three of the pressure/drawdown cycles. Because the safety factor improves with distance into the web, the safety factors plotted in Figure 6 represent the ‘minimum values across the web thickness. As previously noted, the largest drop in safety factor is due to Cavern 15

workovers and only a minor change is noted for Cavern 17 workovers. The reduction in safety factor due to a Cavern 15 workover is abrupt over the 3 month period and could be reduced by shortening the workover period. This is evident by the abrupt stop in the decreasing trend when the cavern is repressurized after the 3 month workover period.

The trends predicted in Figure 6 show drawdowns to initially improve the safety factor of the web. This results from the removal of the more highly strained surface salt in the walls of the caverns. However, because the web thickness is reduced during a drawdown, the rate of strain accumulation increases and the safety factor decreases at a rate faster than its pre-drawdown rate. The time required for the safety factor to equal its pre-drawdown values varies from 0.5 to 2.5 years. Thus the benefit of removing the highly strained wall salt during a freshwater drawdown is relatively short lived and probably will contribute to an overall decrease in cavern life.

The safety factors in Figure 6 drop below 1 after 40 years, suggesting the possibility of failure along the cavern walls in the web. Figure 7 profiles the safety factors through the web at 30, 35, 40, and 45 years. The predicted instability at 40 years is only a skin effect. However, at 45 years, potential failure is predicted through the entire web. It appears that at some time between 40 to 45 years, gross instability of the web is possible under the operating scenarios assumed in this model.

Figure 6 illustrates that the predicted times to failure are heavily dependent upon the pressure and drawdown histories of the caverns. Therefore the times discussed in this report are applicable only to this model and may not represent future cavern behavior, because the future uses and operating pressures of Caverns 15 and 17 are unknown. A better relationship for judging actual web stability may be web thickness, although again, it is recognized that the accumulated strain in a web of a given thickness (and therefore safety factor) will depend upon the pressure and drawdown history of the caverns.

Figure 8 plots the predicted web thickness over time. The predicted web

thickness after 40 years is less than 100 ft. Thus one could speculate that web thickness of less than 100 ft may be inadequate for stability, particularly during a workover or low pressure operation of Cavern 15.

The complexity of the stability/web thickness relationship is illustrated in Figure 8 which shows the workovers of Cavern 15 to produce a slightly thicker web, yet as previously discussed, a less stable web. The web is thickened due to creep which is accelerated during a workover or period of low cavern pressure. Conversely, the drawdowns reduce the size of the web, but initially result in a more stable web.

Thus knowing only the size of a web is not sufficient information for determining its stability. The previous and future pressure/leach times, durations, and magnitudes must be known to make an accurate evaluation. Since this information remains largely unknown, the analyses presented in this report should be considered as generic. The results are more applicable in establishing trends and understanding the mechanics of salt during workovers and leaching. From this, guidance can be provided for the future uses and operation of the caverns.

5.0 CONCLUSION

The stability calculations of the web of salt between Bayou Choctaw Caverns 15 and 17 suggest a compressive failure mode rather than tensile failure as previously thought. Earlier elastic-plastic analyses (Ney, 1979; and Hilton, et al., 1980) predicted tensile failure in the web due to uneven loading of the web. However, these analyses applied instantaneous loads and did not include a creeping constitutive model for the salt. A gradual, more realistic load rate coupled with the creeping constitutive model, which allows stresses to relax, resulted in a compressive stress state (>690 psi) in the web throughout the pressure and drawdown histories simulated. Although the previous analyses differ in the failure mode, both predict potential web instability for thickness of less than 100 ft.

The previous calculations showed the stability of the web to be a function of the differential cavern operating pressures. Currently, the caverns are operated at similar pressures. These analyses show that due to the larger size of Cavern 15 (2.5 times the diameter of Cavern 17) in the web area, the pressure in Cavern 15 dominates the stability of the web and Cavern 17 pressure has little effect on overall web stability. From a stability point of view. maintaining normal pressures in Cavern 15 is more important than operating the caverns as a gallery where both caverns are operated at the same pressure. However, during a workover. it may be prudent to operate the caverns under similar pressures to avoid the possibility of a sudden and uncontrollable pressure at the wellhead should the web fail.

A workover of Cavern 15 causes a significant impact on the stability of the web, whereas a Cavern 17 workover did not. Workovers of Cavern 15 decrease safety factors from 31 to 38 percent, whereas workovers of Cavern 17 only decrease safety factors by 3 to 5 percent. This suggests that if a Cavern 15 workover is required, the pressures in Cavern 17 may be reduced without much impact on the web. Lowering the pressure in both caverns would reduce the risk associated with a large-scale breach of the web that could lead to an abrupt pressurization of Cavern 15 and possibly an uncontrollable well. In contrast, lowering the pressure of Cavern 15 during a Cavern 17 workover is predicted to significantly increase the possibility of web failure.

The dominant behavior of Cavern 15 strongly argues for maintaining high operating pressures in that cavern. shortening or avoiding workovers. and repressurizing the cavern as soon as possible after a workover is complete. Because Cavern 15 appears to control the stabilitv of the web. it is much more important to keep the normal operating pressures up in Cavern 15 than in Cavern 17.

Presently, freshwater cycles that would enlarge the caverns are not recommended (Hogan, 1980). This recommendation is, in general, supported by the web analysis. However, drawdowns have a short-term

benefit. Drawdowns initially improved the web safety factors by removing highly strained salt near the walls of the caverns. For both Cavern 15 and 17, drawdowns immediately improved the safety factors by approximately 20 percent. However, the narrower web that results from a fresh water drawdown creeps faster than before the drawdown, thus the benefit is short-lived, lasting only 0.5 to 2.5 years. If salt failure is anticipated or occurring and is going to cause a problem, it may be beneficial to leach and remove the highly strained and failed salt- but this may be at the cost of overall cavern life.

As previously discussed, the modeling in this report does not simulate the progressive yielding and displacement of failed salt from the web. Further, no attempt was made to simulate or couple the hydrologic aspects. As a result, one can only speculate as to the meaning and consequences of predicted failure. Of concern is whether or not massive pieces of salt will dislodge and perhaps damage a hanging string, and the time and rate at which the caverns will communicate and equilibrate in pressure. An abrupt pressure rise during a workover would be undesirable. Perhaps more likely, the salt will initially shear along a thin part of the web and allow the caverns to slowly 'communicate'. The analysis results suggest the time at which the caverns coalesce (and must be operated as a single cavern) will largely depend upon how often and which of the caverns are exercised in the future.

REFERENCES

Chan, K.S., S.R. Bodner, A.F. Fossum, and D.E. Munson, 1992. "Constitutive Model for Inelastic Flow and Damage Evolution in Solids Under Triaxial Compression," Joint research paper by Southwest Research Institute, San Antonio, TX; RE/SPEC Inc., Rapid City, SD; and Sandia National Laboratories, Albuquerque, NM.

Ehgartner, B.L., 1992. Effects of Cavern Spacing and Pressure on Subsidence and Storage Losses for the US Strategic Petroleum Reserve, SAND91-2575, Sandia National Laboratories, Albuquerque, NM.

Goin, K.L. and D.K. Buchanan, 1986. Test of Department of Energy Strategic Petroleum Reserve Bayou Choctaw Cavern 17, SAND86-0454, Sandia National Laboratories, Albuquerque, NM, April.

Hilton, P.D., J.R. Tillerson, S.E. Benzley, and M.H. Gubbels, 1980. Interaction Effects of Storage Caverns in Salt, SAND79-0732, Sandia National Laboratories, Albuquerque, NM, August.

Hogan, R.G. et al., 1980. Strategic Petroleum Reserve (SPR) Geologic Site Characterization Studies Bayou Choctaw Salt Dome. Louisiana, SAND80-7140, Sandia National Laboratories, Albuquerque, NM.

Krieg, R.D., 1984. Reference Stratigraphy and Rock Properties for the Waste Isolation Plant (WIPP) Project, SAND83-1908, Sandia National Laboratories, Albuquerque, NM.

Munson, D.E., 1979. Preliminary Deformation-Mechanism Map for Salt (with Application to WIPP), SAND70-0076, Sandia National Laboratories, Albuquerque, NM.

Munson, D.E. 1989. "Proposed New Structural Reference Stratigraphy, Law. and Properties", Internal technical memorandum to distribution, 8/22/89, Sandia National Laboratories, Albuquerque, NM.

Munson, D.E. 1992. 'Mechanical Parameters for Volume 3, SAND92-0700.' Internal Memo to M.S. Tierney, dtd 10/26/92, Sandia National Laboratories, Albuquerque, NM.

Munson, D.E. and P.R. Dawson, 1979. Constitutive Model for the Low Temperature Creep of Salt (with Application to WIPP), SAND79-1853, Sandia National Laboratories, Albuquerque, NM.

Munson, D.E., A.F. Fossum, and P.E. Senseny, 1989a. Advances in Resolution of Discrepancies Between Predicted and Measured In Situ WIPP Room Closure, SAND88-2948, Sandia National Laboratories, Albuquerque, NM.

Munson, D.E., A.F. Fossum, and P.E. Senseny, 1989b. Approach to First Principles Model Prediction of Measured WIPP In Situ Room Closure in Salt, SAND88-2535, Sandia National Laboratories, Albuquerque, NM.

Neal, J.T., T.R. Magorian, and Acres International Corp, in prep. Strategic Petroleum Reserve (SPR) Additional Geologic Site Characterization Studies Bayou Choctaw Salt Dome, Louisiana, SAND92-2284, Sandia National Laboratories, Albuquerque, NM.

Ney, J.F., 1979. "Cavern 15-17 Depressurization," Memo to W. Mazurkiewicz, DOE SPR PMO from Sandia National Laboratories, November 27.

Preece, D.S. and W.R. Wawersik, 1984. "Leached Salt Cavern Design Using a Fracture Criterion for Rock Salt," SAND83-2345C, Sandia National Laboratories, Albuquerque, NM. Also, Proceedings of 25th U.S. Symposium on Rock Mechanics, June 1984, Northwestern University.

Ratigan, J.L. and K.L. DeVries, 1989. "Potential Geomechanics Problems Resulting From Closelv Spaced Storage Wells in Dome Salt," SPE 19085, Society of Petroleum Engineers, SPE Gas Technology Symposium, Dallas, TX June 7-9.

RE/SPEC, 1989. Documentation of SPECTROM-32: A Finite-element Thermomechanical Stress Analvsis Program, RE/SPEC Inc., Rapid City, SD.

SPR, 1987. Design Criteria- Level III. DOE U.S. Strategic Petroleum Reserve, New Orleans, LA.

Wawersik, W.R. and D.H. Zeuch, 1984. Creep and Creep Modeling of Three Domal Salts-- A Comprehensive Update, SAND84-0568, Sandia National Laboratories, Albuquerque, NM.

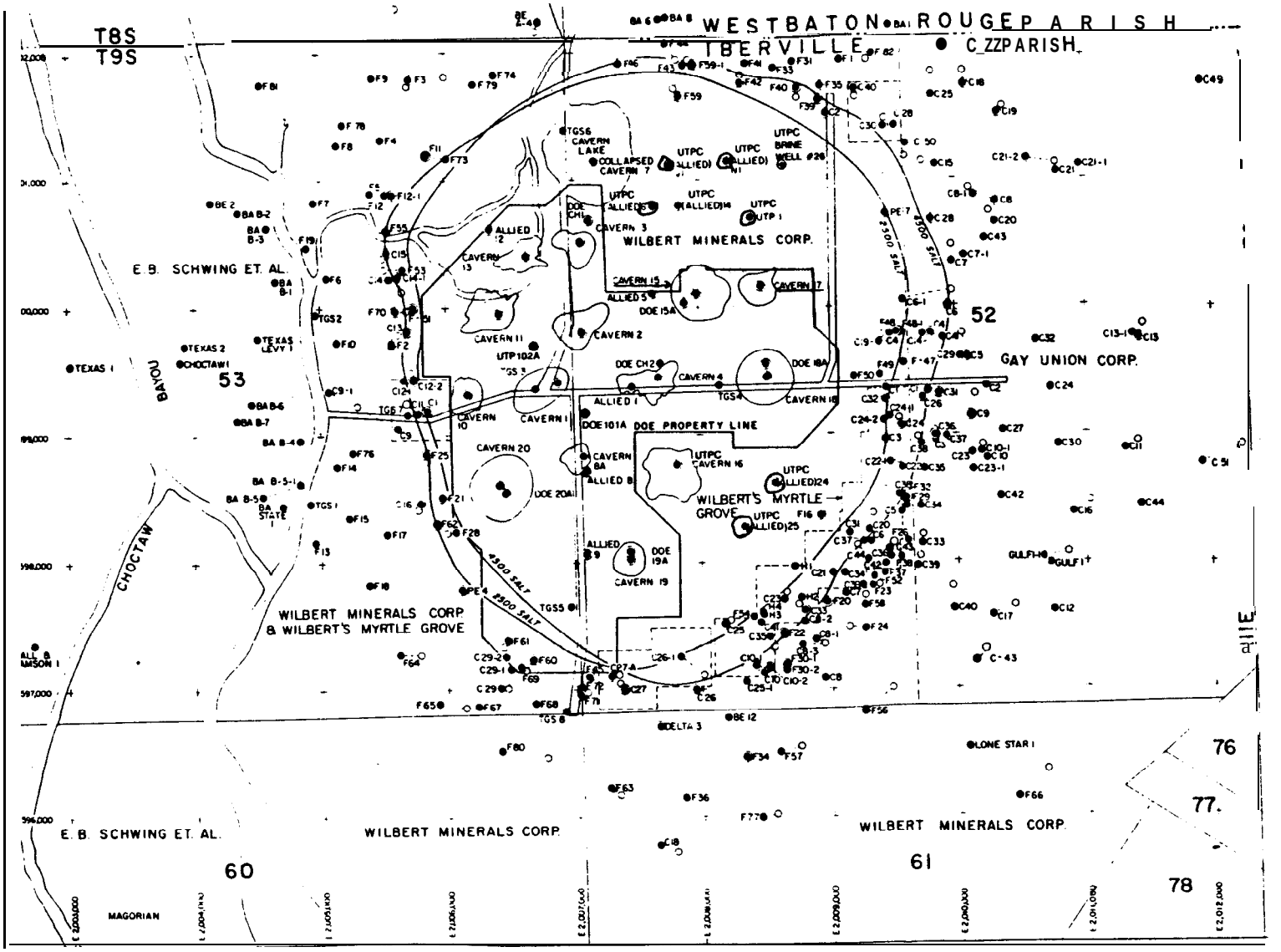

Figure 1. Site Layout at Bayou Choctaw Showing Cavern Outlines and Top of Salt Contours (ft. below surface). Caverns 15 and 17 are located along the North-East property boundary.

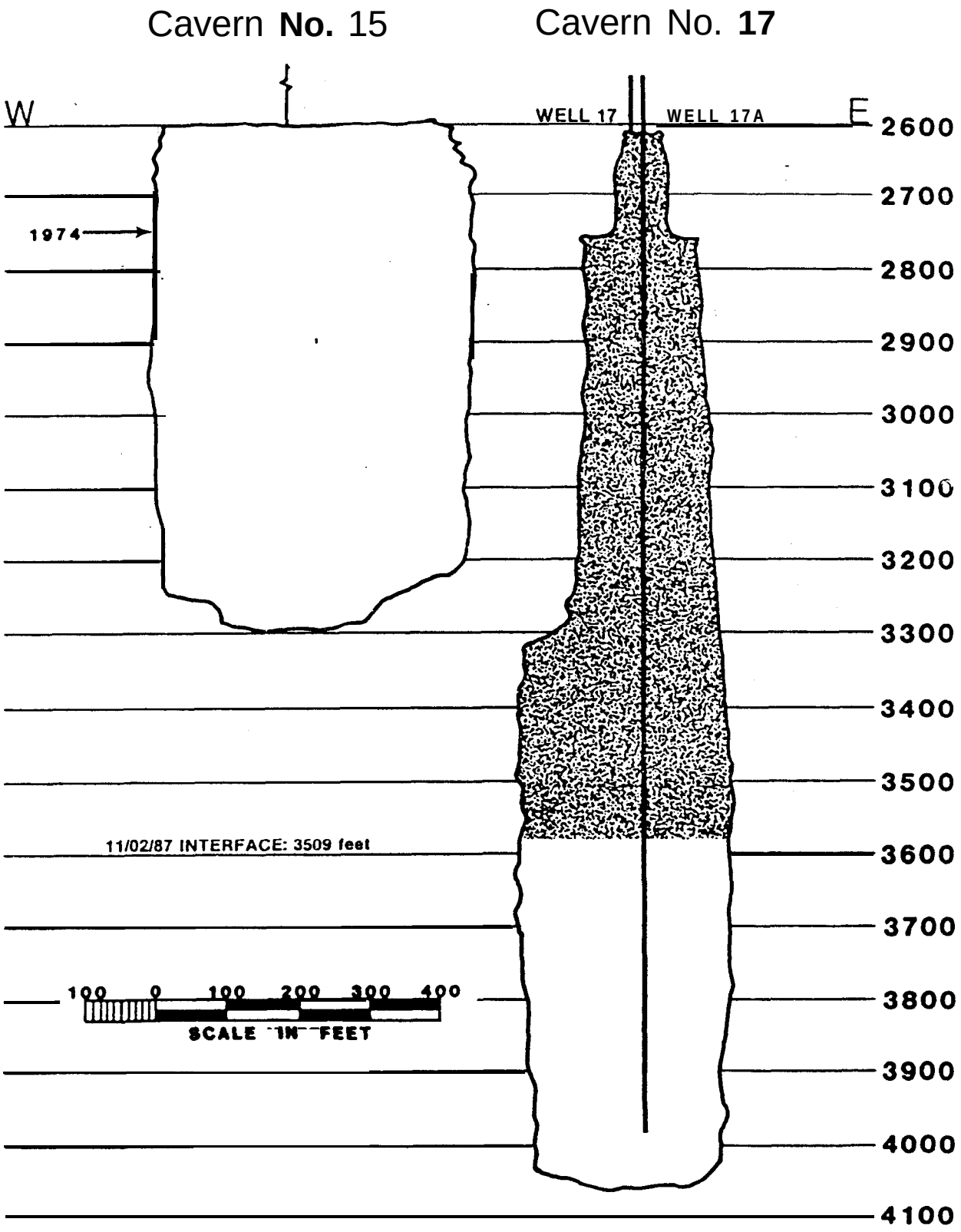

Figure 2. Vertical Cross-Section of Caverns 15 and 17.

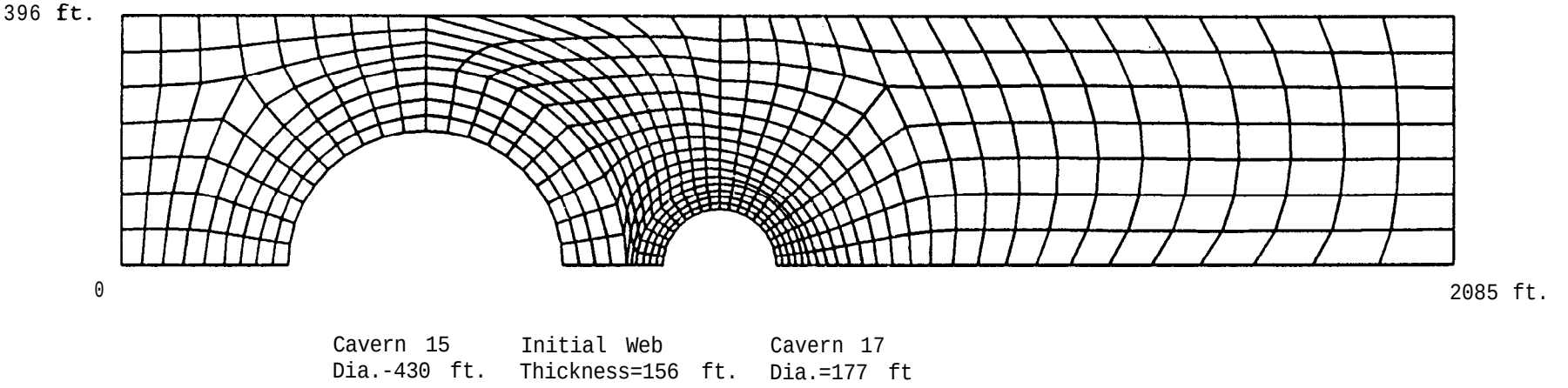

Figure 3. Finite-Element Mesh Used in Web Analysis for Caverns 15 and 17. Top, bottom, and left sides are planes of symmetry. Right side of mesh represents the edge of the dome with a constant lithostatic pressure applied.

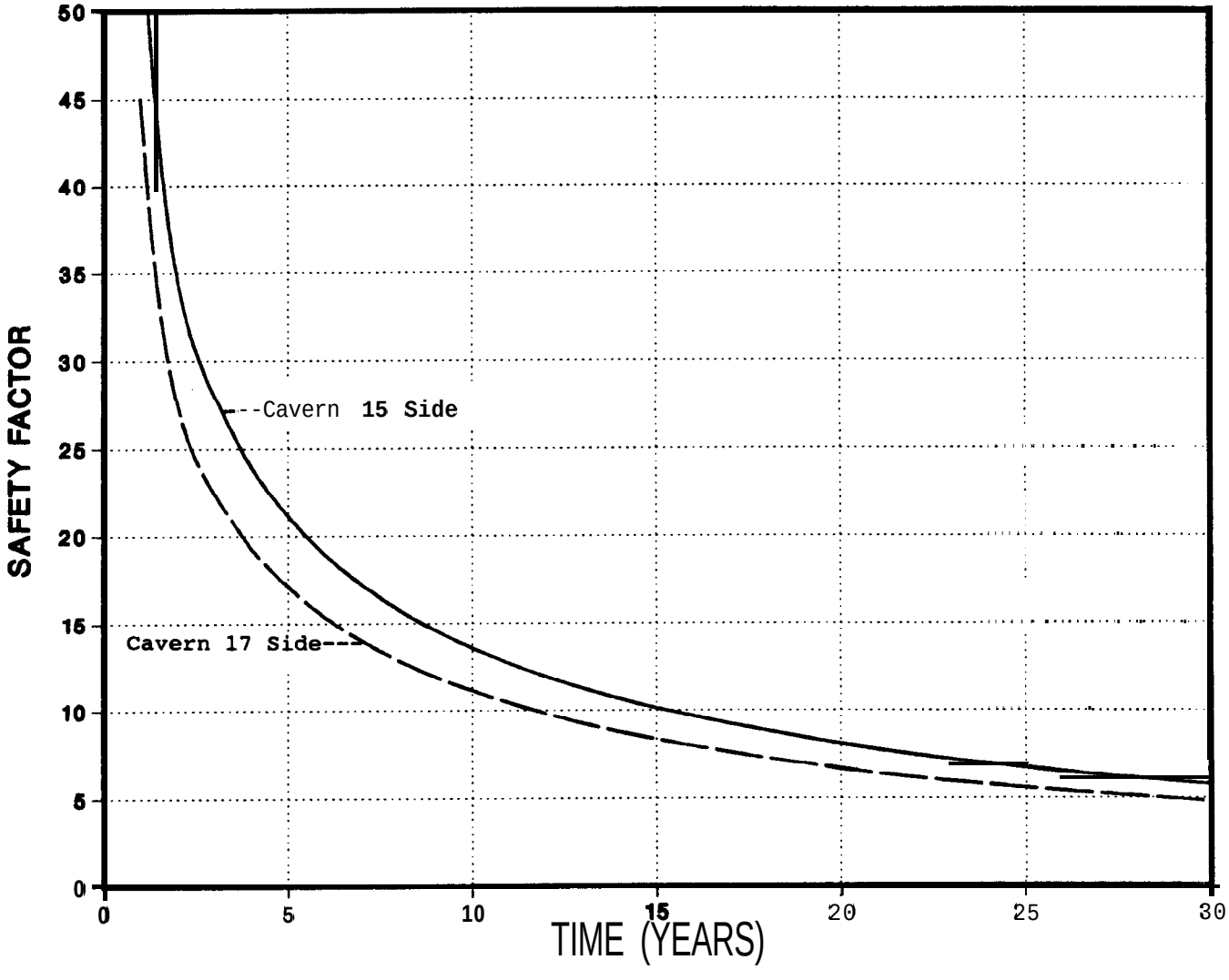

Figure 4. Predicted Factors of Safety for Salt Stability at Sides of Web During The Initial 30 Years of Simulation. The past operational history of the caverns is approximated during the initial 30 years of simulation as a constant pressure.

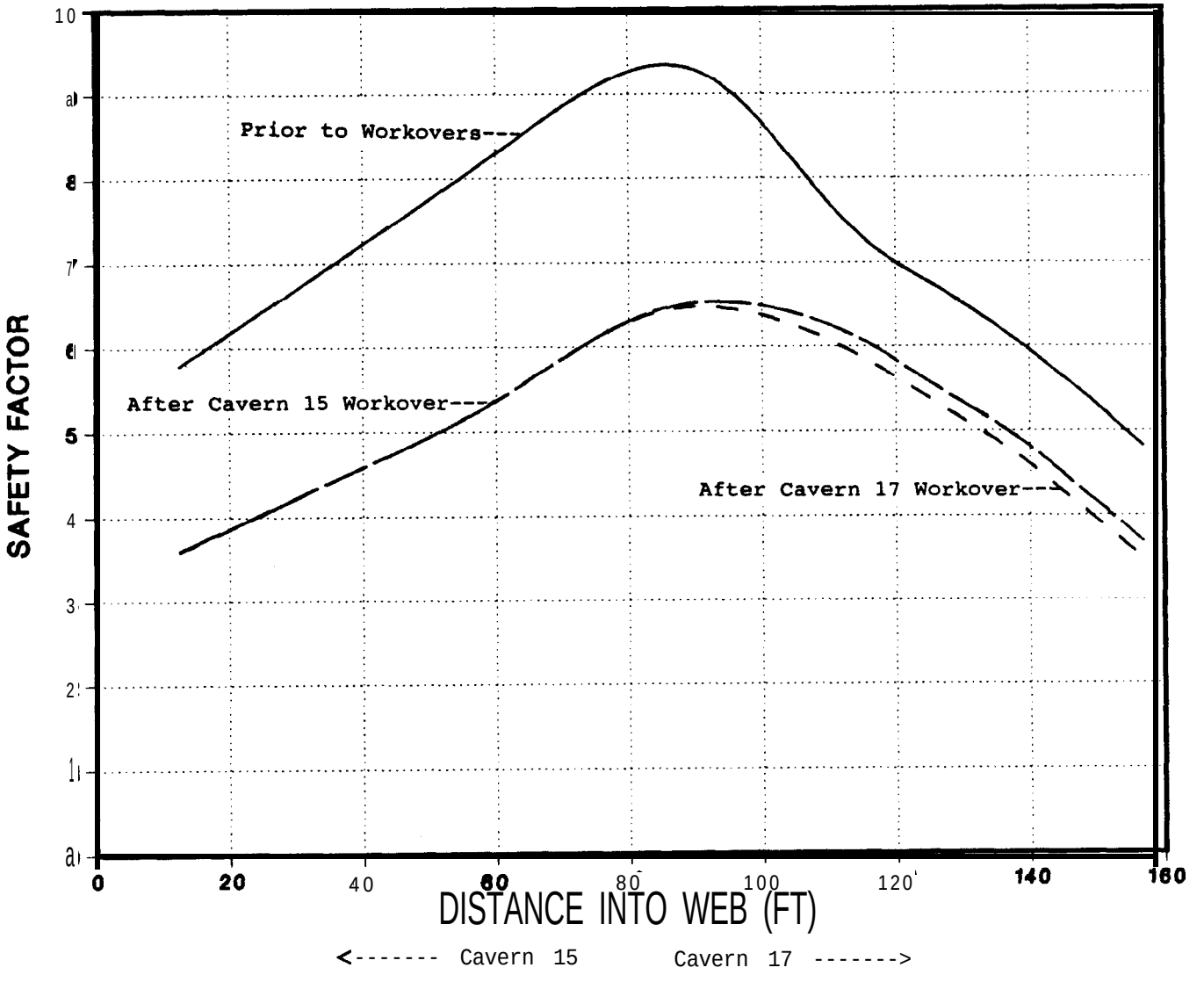

Figure 5. Predicted Distribution of Safety Factors in Web at 30 Years, 30.25 Years (End of Cavern 15 Workover), and 30.75 Years (End of Cavern 17 Workover). The initial 30 years of simulation approximate the historic operations of the caverns.

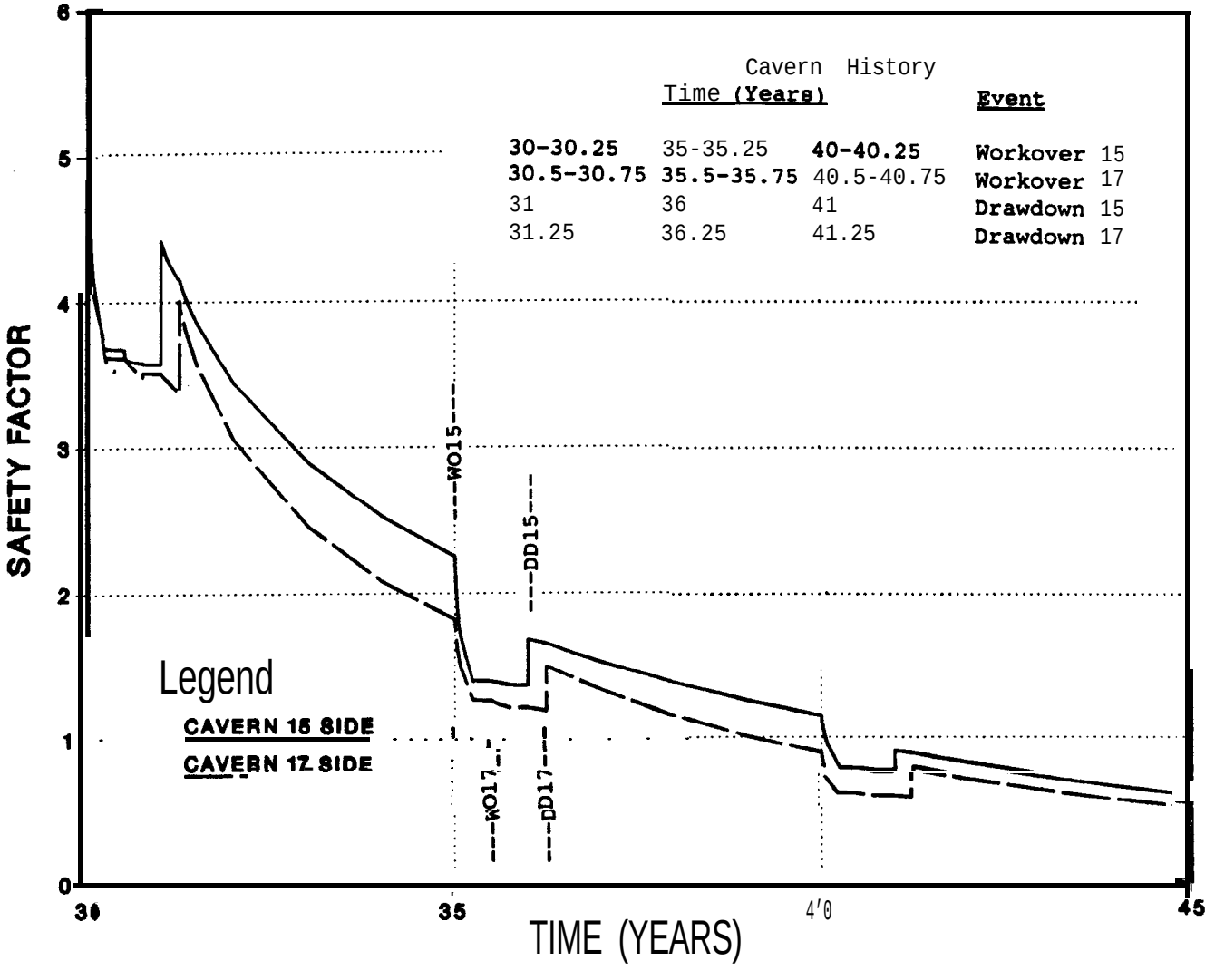

Figure 6. Predicted Factors of Safety at Sides of Web From 30 to 45 Years Showing Effects of Workovers and Drawdowns on Web Stability. The initial 30 years of simulation approximate the historic operations of the caverns.

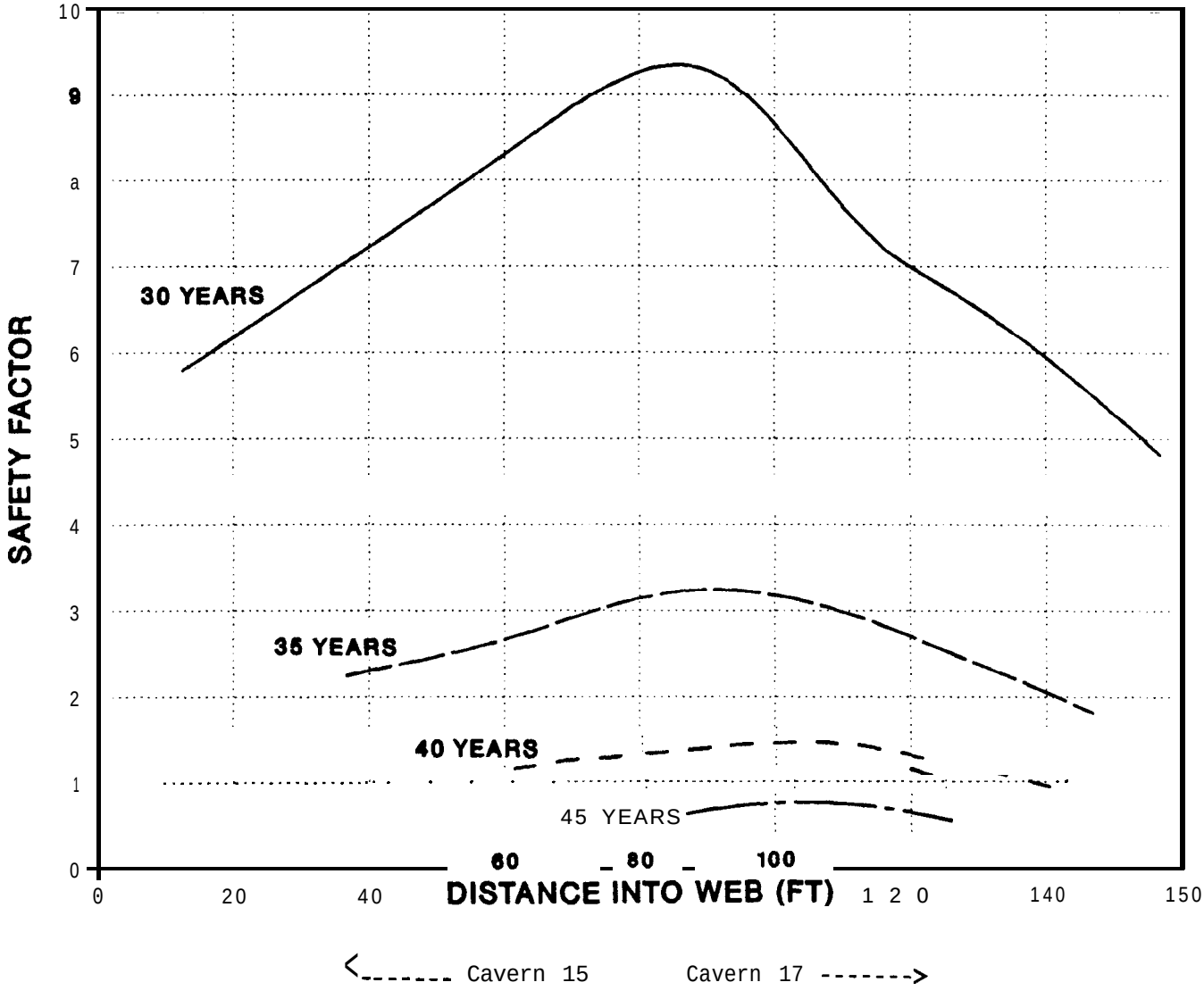

Figure 7. Predicted Distribution of Safety Factors in Web at 30, 35, 40, and 45 Years. The initial 30 years of simulation approximate the historic operations of the caverns.

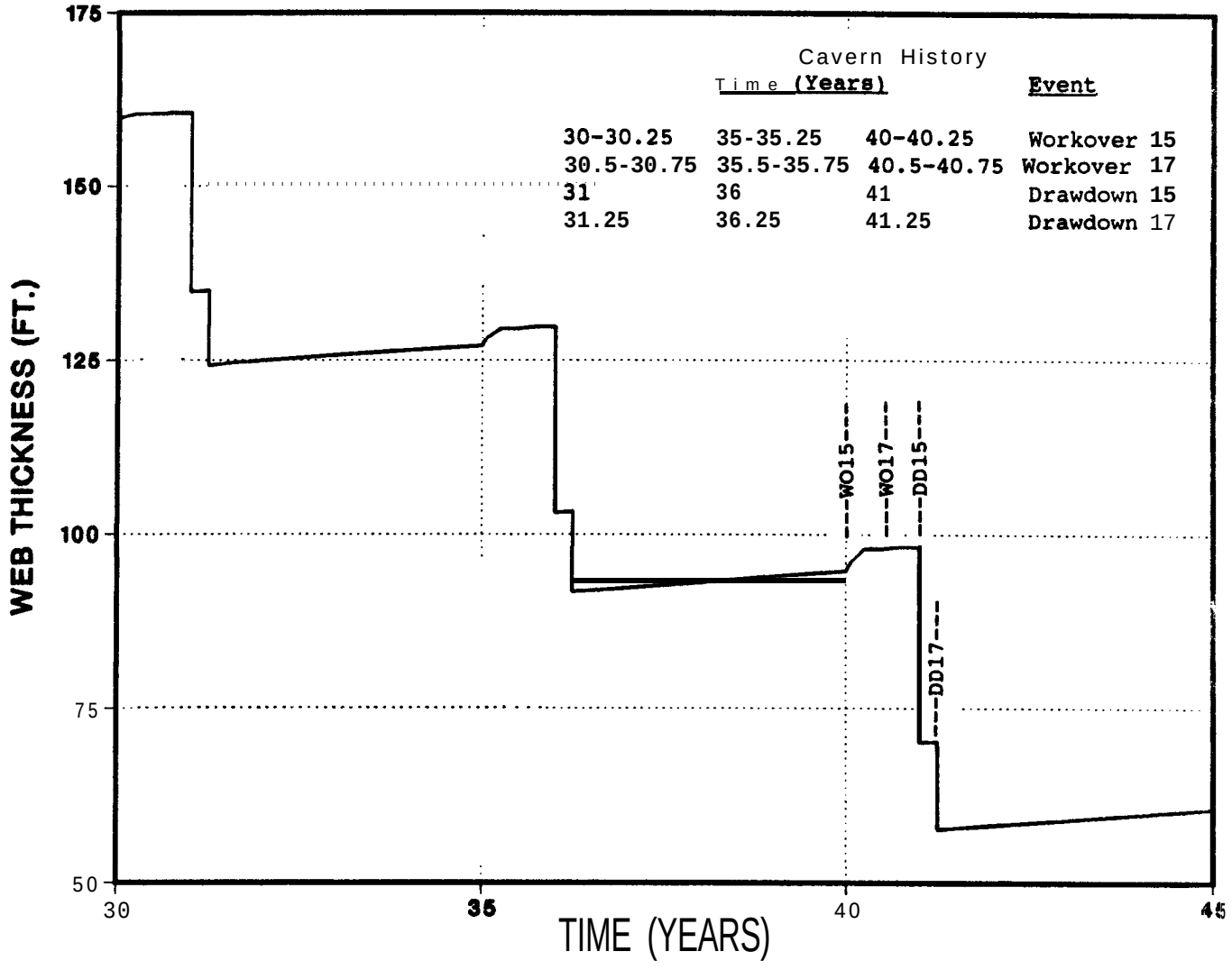

Figure 8. Predicted Web Thickness During Periods of Workovers and Drawdowns. The initial 30 years of simulation approximate the historic operations of the caverns.

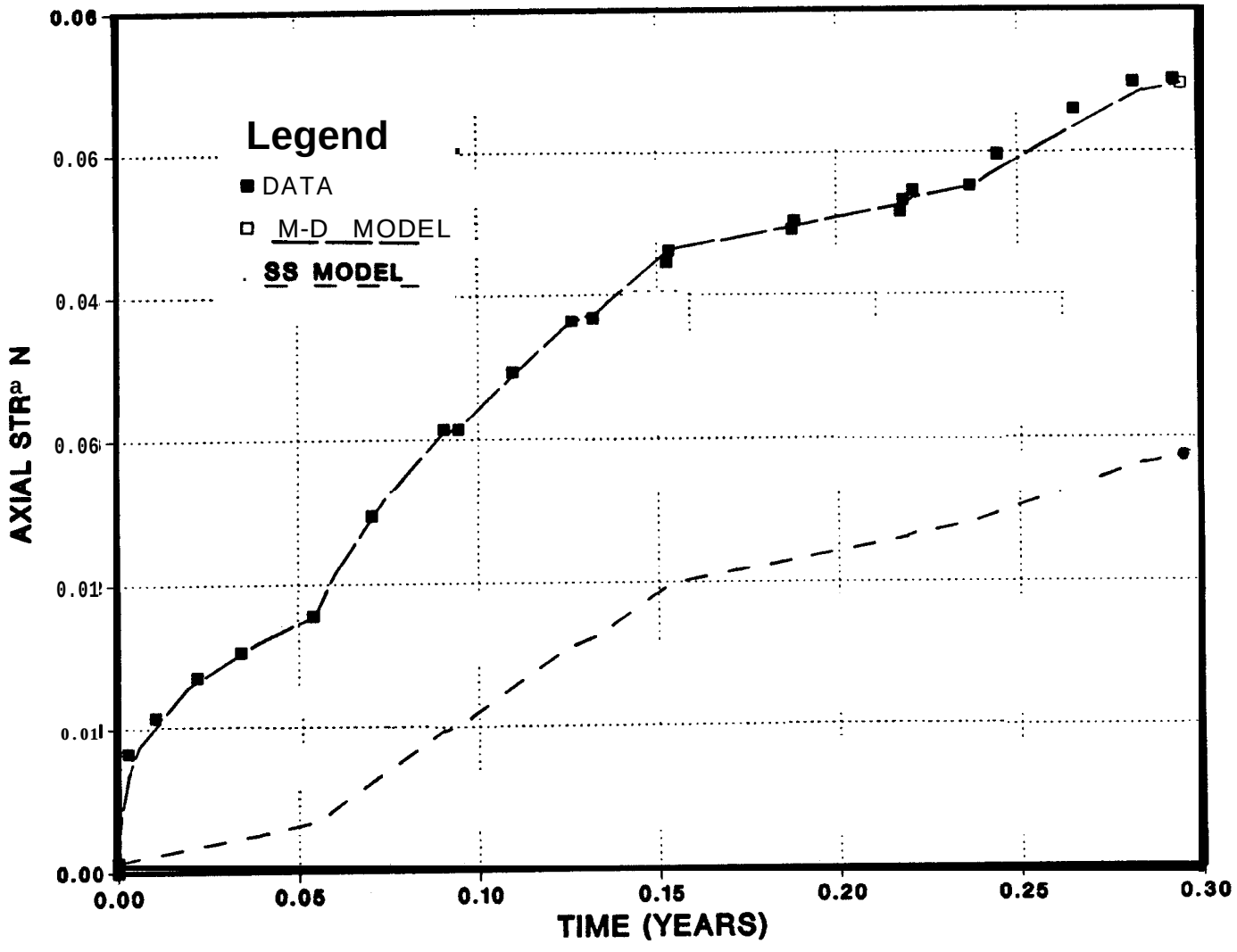

Figure A. Comparison of Measured Axial Strains from BC Creep Test QG4N with Predictions from the Munson-Daweon (M-D) Model. Also shown is the predicted strains assuming only eteady state (SS) creep. The differece between M-D and SS predictions is due to transient creep.

DISTRIBUTION

US DOE SPR PMO (5)
900 Commerce Road East
New Orleans, LA 70123
Attn: J. W. Kunkle, PR-622
R. Myers, PR-622
L. Rousseau, FE-443
TDCS (2)

US DOE SPR (2)
1000 Independence Avenue SW
Washington, DC 20585
Attn: D. Johnson
D. Smith

Boeing Petroleum Services (3)
850 S. Clearview Parkway
New Orleans, LA 70123
Attn: K. Wynn
T. Eyerman

Boeing Petroleum Services (1)
60825 Hwy. 1148
Plaquemine, LA 70764
Attn: Matt Slezak

RE/SPEC Inc. (1)
3824 Jet Drive
Rapid City, SD 57709
Attn: Joe Ratigan

Sandia Internal:
1561 H. S. Morgan
1561 E. L. Hoffman
6000 D. L. Hartley
6100 R. W. Lynch
6112 D. S. Preece
6113 J. K. Linn (10)
6113 S. J. Bauer
6113 B. L. Ehgartner (10)
6113 T. E. Hinkebein
6113 P. S. Kuhlman
6113 R. V. Matalucci
6113 J. T. Neal
6113 J. L. Todd
6113 S. T. Wallace
6117 W. R. Wawersik
6121 D. E. Munson
8523-2 Central Technical Files
7141 Technical Library (5)
7613-2 Document Processing (10)
For DOE/OSTI
7151 Technical Publications (1)